

## Biosynthesis of Silver Nanoparticles Using the Compound Curvularin isolated from the Endophytic Fungus *Epicoccum Nigrum*: Characterization and Antifungal activity

Sobhy I. I. Abdel-Hafez<sup>1</sup>, Nivien A. Nafady<sup>1</sup>, Ismail R. Abdel-Rahim<sup>1,\*</sup>, Abeer M. Shaltout<sup>2</sup>, José-Antonio Daròs<sup>3</sup> and Mohamed A. Mohamed<sup>1,2,3</sup>

<sup>1</sup>Botany and Microbiology Department, Faculty of Science, Assiut University, Assiut 71516, Egypt.

<sup>2</sup>Plant Pathology Research Institute, Agricultural Research Center, Giza 12655, Egypt.

<sup>3</sup>Instituto de Biología Molecular y Celular de Plantas (Consejo Superior de Investigaciones Científicas - Universidad Politécnica de Valencia), Avenida de los Naranjos, 46022 Valencia, Spain.

Received: 5 Mar. 2017, Revised: 12 Apr. 2017, Accepted: 17 Apr. 2017.

Published online: 1 May 2017.

**Abstract:** A simple new green method for the synthesis of silver nanoparticles (AgNPs) using the anti-oxidant compound curvularin isolated from the endophytic fungus *Epicoccum nigrum* ASU1 is reported for the first time in this article. The present work describes a one-step functionalization of AgNPs using compound curvularin as a reducing and stabilizer agent. The AgNPs capped curvularin were characterized by UV-vis spectroscopy, Fourier transform infrared (FT-IR) spectroscopy, X-ray diffraction (XRD), selected area electron diffraction (SAED), energy dispersive X-ray spectroscopy (EDX), and high-resolution transmission electron microscopy (HR-TEM). The results showed the formation of high purified spherical AgNPs with an average size of 37 nm. The FT-IR results suggested that both hydroxyl and carbonyl functional groups in curvularin are responsible for the reduction of the Ag<sup>+</sup> ions and stabilizing AgNPs. The AgNPs showed potent antifungal activity at various extends compared to curvularin alone against the phytopathogenic fungus *Alternaria solani*. These findings emphasise that such biocompatible green nanoparticles, thanks to their potent antifungal activities, may be applied as new bio-fungicides against various plant pathogenic fungi in the field of plant protection and plant disease management.

**Keywords:** Silver nanoparticles, Biosynthesis, Curvularin, *Epicoccum nigrum*, Endophytes, Antifungal activity.

## 1 Introduction

Nanotechnology, one of the most active areas of research in modern material sciences, focuses on the development of synthetic and natural systems for the production of structures and materials at nanoscale [1,2]. Nanoparticles exhibit completely unique physical, chemical and biological properties as compared to large particle of the bulk material [3]. These unique properties arise due to their small size and large specific surface area. Hence, the metal nanoparticles, particularly silver nanoparticles (AgNPs), are emerging as one of the fastest growing nanomaterials, playing an important role in pharmaceutical, industrial and biotechnological applications [4,3]. Recently, they have been shown to have potential application against different diseases caused by bacteria, fungi, and viruses [5], high sensitivities in the bio-molecular detection and diagnostic [6], therapeutic activity [7], catalytic activity in chemical reactions and bio-labeling [8], micro-electronics fields [9], optical receptors [10], biosensors [11], signal enhancers in SERS-based enzyme immunoassay [12], and many other

engineering and biomedical applications [13,14]. A multitude of chemical and physical methods have been established to synthesize AgNPs, including conventional chemical reduction utilising sodium borohydride, citrate, ascorbate and hydrazine as reducing agents [15,16], spray pyrolysis [17], physical vapor deposition [18], and irradiation route [19]. Since most processes described so far are associated with high energy consumption or involve toxic chemicals they are not considered environmentally benign. Today, synthesis of noble AgNPs using ecofriendly biological approaches like plants [20,21], agricultural wastes [22], and microorganisms [23] has received major attention as alternatives to chemical and physical methods. Fungi are considered the best option compared to other eukaryotes [24]. This comes from the vast repertoire of proteins, enzymes, and other bioactive secondary metabolites produced from those microbes that possess redox capacity, and can be exploited in the biosynthesis process, thus increasing productivity. In addition, fungi are

\* Corresponding author E-mail: [ismailramadan2008@gmail.com](mailto:ismailramadan2008@gmail.com)

simple to deal with in the laboratory and at an industrial scale. The process can be easily scaled up and be economically viable, with the possibility of easy covering large surface areas by suitable growth of mycelia. Furthermore, downstream processing would be much simpler using fungi [25,26]. Recently, a green route based on natural pure biological molecules such as chitosan, starch and tannic acid has been successfully used as reducing capping agents for the synthesis of AgNPs and controlling their properties [27-31]. The biological molecules can easily undergo highly controlled, hierarchical assembly [32], which makes them suitable for the development of reliable and ecofriendly processes for metal nanoparticle synthesis [33]. Furthermore, these methods are cheap, rapid and efficiently produce single atoms or molecules with a wide variety of shapes (spheres, prisms or plates) at the nano scale level. Our aim in the present work was to synthesize of AgNPs using biomolecules, more specifically the compound curvularin, derived from the endophytic fungus *Epicoccum nigrum* ASU1 to be utilized as reducing and chelating agent in the biosynthesis process. Also, evaluate the fungicidal activity of curvularin and biosynthesized AgNPs the phytopathogenic fungus *Alternaria solani*, the causal agent of tomato early blight disease..

## 2 Materials and Methods

### 2.1 Instrumentation

Thin layer chromatography (TLC) was performed on plates pre-coated with Si 60 F254 (Merck, Darmstadt, Germany). Column chromatography (CC) was carried out on silica gel (0.2 mm silica gel 60 F254 pre-coated alumina; Merck, Darmstadt, Germany). The isolated compound was detected spectrophotometrically. For HPLC analysis, sample was injected into an HPLC system with a photodiode-array detector (Dionex, Munich, Germany). Routine detection was at 254 nm in aqueous methanol. Mass spectra (ESI mass) were obtained on a Thermofinnigan LCQ DECA mass spectrometer coupled to an Agilent 1100 HPLC system equipped with a photodiode array detector. <sup>1</sup>H NMR and <sup>13</sup>C NMR spectra (chemical shifts in ppm) were recorded on a Bruker ARX-400, DRX 500 or DMX 600 spectrometers using standard Bruker software, and DMSO-*d*<sub>6</sub> or MeOH-*d*<sub>4</sub> was used as a solvent. For spectral simulation, the Mest ReC software package (version 4.9.9.9) was used (Mestrelab Research, Santiago de Compostela, Spain). Solvents were distilled before use and spectral grade solvents were used for spectroscopic measurements.

### 2.2 Fungal source and medium of isolation

Fresh healthy leaves of tomato plants (*Solanum lycopersicum* L.) were collected from Aswan Governorate, Egypt in April 2014. The collected samples were packed directly into sterilized polyethylene bags and transferred to

mycological laboratory. Potato dextrose agar (PDA) medium containing 66.7 mg L<sup>-1</sup> rose bengal and 250 mg L<sup>-1</sup> streptomycin was used for isolation of endophytic fungi [34].

### 2.3 Isolation and purification of the endophytic fungi

Plant materials were thoroughly washed with running tap water to remove dust and spores deposited from air, washed several times with sterilized distilled water and then dried thoroughly using sterilized paper towel. Endophytic fungi were isolated through surface sterilization technique [35]. Tomato leaves were sterilized using 75% ethanol for 1 min, followed by immersion in 1% sodium hypochlorite for 5 min and again in 75% ethanol for 30s. Leaves were washed by sterilized distilled water, dried thoroughly between sterilized paper towel and cut into segments (1 cm<sup>2</sup>) in a laminar air flow chamber. Five leaf segments were placed on the surface of PDA medium. Five plates were used for this sample and then they were incubated at 25°C for 3 days. Fungi emerging out of the plant tissues were purified using hyphal tip technique described by Sinclair, Dhingra [36].

### 2.4 Identification of endophytic fungus *Epicoccum nigrum* ASU1

The isolated tested fungus (*Epicoccum nigrum* ASU1) was firstly identified according to morphological and microscopic characteristics recorded in different mycological keys [37,38]. Consecutively, the identification was confirmed at molecular level using PCR amplification of the ribosomal internal transcribed spacer (ITS) region with universal primers ITS1 and ITS4.

#### 2.4.1 DNA extraction

*Epicoccum nigrum* ASU1 was grown for five days in 250 ml Erlenmeyer flasks containing 100 ml potato dextrose broth under continuous agitation (125 rpm) at 28°C. Fungal pellets were collected by vacuum filtration through a piece of filter 0.45 μm (Seitz), washed with distilled water and frozen at -80°C. Frozen mycelia (100 mg) were grounded in the presence of liquid nitrogen with a mortar and pestle and then mixed with 1 ml of 4 M guanidinium thiocyanate, 0.1 M sodium acetate pH 5.5, 10 mM ethylenediaminetetraacetic acid (EDTA), 0.1 M 2-mercaptoethanol. Extract was clarified by centrifugation and the supernatant loaded into a spin silica gel column (Wizard Plus SV Minipreps DNA Purification, Promega, USA). Column was washed with 70% ethanol, 10 mM sodium acetate pH 5.5 and DNA eluted with 50 μl of 20 mM Tris-HCl, pH 8.5.

#### 2.4.2 Ribosomal ITS DNA amplification and sequencing

Ribosomal ITS was amplified by PCR using primer pair ITS1 (5'-CTTGGTCATTTAGAGGAAGTAA-3') and ITS4 (5'-TCCTCCGCTTATTGATATGC-3') [39]. Fungal DNA (1  $\mu$ L) was amplified in a 20- $\mu$ L reaction with 0.4 U Phusion DNA polymerase (Thermo Scientific) in the presence of 0.2 mM dNTPs, 3% dimethyl sulfoxide, 0.5  $\mu$ M each primer and HF buffer (Thermo Scientific). Reaction consisted of an initial denaturation for 30 s at 98°C, followed by 30 cycles of 10 s at 98°C, 30 s at 55°C and 30 s at 72°C, and a final extension of 10 min at 72°C. PCR products were separated by electrophoresis in a 1% agarose gel run for 75 min in buffer TAE (40 mM Tris, 20 mM sodium acetate, 1 mM EDTA, pH 7.2) and visualized using a UV illuminator after ethidium bromide staining. The PCR product corresponding to ribosomal ITS, according to electrophoretic migration, was eluted from the gel using spin silica columns (DNA Clean & Concentrator, Zymo Research). Both strands of amplified ribosomal ITS DNA were sequenced using primers ITS1 and ITS4. The consensus sequence was used to search for homologous sequences using the BLAST search program at National Center for Biotechnology Information (NCBI; <http://www.ncbi.nlm.nih.gov>). Multiple sequence alignment and molecular phylogeny were performed using CLUSTALW program (<http://clustalw.ddbj.nig.ac.jp/top-eh.html>). The phylogenetic tree was constructed with referential *Epicoccum nigrum* strains from GenBank (GU934519, KF881763, HQ115657, JF440590, AF455403, EU272494, KC867291) and using MegAlign software (DNASar 5.01).

## 2.5 Extraction of fungal secondary metabolites

*Epicoccum nigrum* ASU1 was cultivated on Erlenmeyer flasks (250 mL) containing 100 mL of potato dextrose broth and then incubated for 10 days at 25°C under shaking (150 rpm/min) using an orbital shaker (Thermo Forma, Refrigerated). The fungal pellets were discarded, while the culture broth was filtered through Whatman no.1 filter paper. The culture broth was extracted three times with equal volume of ethyl acetate using separation funnel. Then the organic layers were combined, dried through anhydrous sodium sulfate and filtered. The solvent was evaporated using a rotary evaporator (Heidolph, Kehlheim, Germany).

## 2.6 Isolation and identification of curvularin

One gram of dried crude extract was subjected to silica column chromatography (0.2 mm silica gel 60 F254 pre-coated alumina, Merck, Darmstadt, Germany), eluted with hexane, ethyl acetate and methanol to yield four main fractions (100 mL each). Each fraction was concentrated under vacuum, gently evaporated and dried under nitrogen gas stream. The fraction1 (100.65 mg), eluted in 90% methanol, was ultra-sonicated for 10 min and purified using a 0.2  $\mu$ L disposable filter. Curvularin (3.81 mg) was isolated and purified from fraction 1 by a Sephadex LH-20 column using methanol as solvent system. Curvularin was

characterized as brownish spots on a silica gel plate [Rf 0.6, benzene-EtOAc, 3: 2] when sprayed with a 2% solution of vanillin in 100% sulfuric acid. The final purification was performed by multiple cycles run with an Agilent 1260 semi-preparative HPLC system (Phenomenex, Torrance, CA, USA). Forty  $\mu$ L of crudely purified metabolites were injected into the HPLC column using at a flow of 5 mL/min with a linear water-acetonitrile gradient. The gradient started at 0% acetonitrile and reached 60% in 10 min, which were held for 1 min before reverting to 0% acetonitrile.

### 2.6.1 Structural verification

The structure of one of the isolated compound (curvularin) was determined by nuclear magnetic resonance (NMR) spectroscopy on a Bruker AVIII-600 spectrometer (Bruker, Karlsruhe, Germany). Approximately 5  $\mu$ g of the compound were dissolved in 600  $\mu$ L of deuterated chloroform ( $\text{CDCl}_3$ ) and were analysed with  $^1\text{H}$  and  $^{13}\text{C}$  at 291 K. Spectra were recorded and analysed with TopSpin 3.2 (Bruker). Residual solvent signals were used as internal standards (reference signal). The observed chemical shift ( $\delta$ ) values were given in ppm and the coupling constants (J) in Hz.

## 2.7 Biosynthesis of AgNPs using extracellular curvularin

For biosynthesis of AgNPs using the isolated compound, a silver nitrate solution (1mM in deionized water, 300  $\mu$ L) was mixed with curvularin compound (0.5 mM in deionized water, 100  $\mu$ L). The final volume of mixture was adjusted to 1mL with deionized water while stirring at room temperature. The reaction mixture was then incubated at 25°C in the dark to avoid photochemical reduction. The reduction of  $\text{AgNO}_3$  in the solution and the formation of AgNPs were preliminarily confirmed by visually observing the colour change that took place from pale white to reddish brown, as further confirmed by UV-vis spectroscopy.

## 2.8 Characterization of AgNPs

### 2.8.1 UV-Vis spectroscopic analysis

The reduction of silver nitrate in the solution and the formation of AgNPs was preliminarily confirmed by visual observation of color change from pale white to reddish brown and further confirmed by UV-Visible spectroscopy. A small aliquot (2 mL) of the colored suspended particles was taken in a quartz cuvette and observed for wavelength scanning ranging between 300-800 nm at different time intervals with distilled water as a reference. PerkinElmer Lambda 950 UV/Vis spectrometer was used for UV visible spectroscopy. The colored mixture was then centrifuged at 10,000 rpm for 20 min and washed three times with deionized distilled water, and finally dried at 60°C.

### 2.8.2 Dynamic light scattering (DLS)

The dynamic light scattering (DLS) or zeta-sizer is a technique used to measure the size and size distribution of very small particles dispersed in a liquid. To estimate the particle size, a dilute suspension of nanoparticles was prepared in deionized water and sonicated for removing aggregation at 35 °C for 20min and subjected to DLS analysis. The average particle size and zeta potential of nanoparticles were estimated using a Zetasizer, Nano-ZS90 system (Malvern Inc., Malvern, UK).

### 2.8.3 High resolution transmission electron microscopy (HR-TEM)

For HR-TEM measurements, the sample solution was pipetted onto a carbon-coated copper grid (carbon type-B, 300 mesh, Ted Pella, Inc., Redding, CA, USA). The sample-loaded grid was air dried under vacuum desiccation for 3 h. The TEM micrograph images were recorded on JEOL instrument 1200 EX instrument on carbon coated copper grids operated at an accelerating suitable voltage (kV). The clear microscopic views were observed and documented in different range of magnifications. Additionally, selected area electron diffraction (SAED) of the nanoparticles was also analysed.

### 2.8.4 X-ray diffraction analysis (XRD) and Energy Dispersive X-ray photometric analysis (EDX)

X-ray diffraction (XRD) analysis was conducted to get information about the crystalline nature of the formed AgNPs. A film of the biologically synthesized AgNPs were cast into glass slides and subjected to X-ray diffraction analysis carried out using Phillips PW 1830 instrument Powder (Phillips, USA). The operating voltage of 40 kV and current of 30 mA with Cu  $\alpha$  radiation of 0.1541 nm wavelength, in the  $2\theta$  range 10-80° angle [40]. The EDX analysis was performed to identify the elemental composition of the biosynthesized AgNPs using INCA Energy TEM 200 with the JEOL analysis software.

### 2.8.5 Fourier transform infrared spectroscopy (FTIR)

FTIR analysis of the dried AgNPs was carried out through the KBr pellet (FTIR grade) method in 1:100 ratio and spectrum was recorded using Jasco FT/IR-6300 Fourier transform infrared spectrometer equipped with JASCO IRT-7000 Intron Infrared Microscope using transmittance mode operating at a resolution of 4  $\text{cm}^{-1}$ (cm21) (JASCO, Tokyo, Japan) [41].

## 2.9 Antifungal assay of AgNPs

The antifungal activity of AgNPs was tested by the agar dilution method. Plates were supplemented with three concentrations of biogenic AgNPs (5, 10, and 20 ppm). A disc (1.5 cm) of mycelial growth of the phytopathogenic

fungus *Alternaria solani* causing tomato early blight disease, taken from the edge of a 6-day-old fungal culture, was placed in the centre of each plate. The inoculated plates were then incubated at 25°C for 8 days. The efficacy of AgNPs treatment was then evaluated by measuring the radial growth of fungal colonies [42]:

$$\text{Inhibition rate (\%)} = R - r / R \times 100$$

Where,  $R$  is the radial growth of the fungal hyphae on the control plate and  $r$  is the radial growth of the fungal hyphae on the plate supplemented with AgNPs. All experiments were conducted in triplicate under sterile conditions.

## 3 Results

### 3.1 Identification of endophytic fungi

In this study, twelve different endophytic fungi were isolated from 50 leaf samples of healthy tomato plants. Of these, eight fungal species were identified as *Alternaria alternata*, *Aspergillus terrus*, *Chaetomium globosum*, *Cladosporium cladosporioides*, *Cladosporium herbarum*, *Epicoccum nigrum*, *Fusarium oxysporum* and *Trichoderma harzianum*. On the other hand, four endophytic fungi were sterile mycelia and did not form reproductive structures (conidia and conidiophores), which were recovered in frequencies up to 6%. The most prominent species was *Epicoccum nigrum* Link (*syn. E. purpurascens* Ehrenb. ex Schlecht), which showed 30% colonization frequency (Table 1).

**Table 1:** Endophytic fungi isolated from 50 samples of healthy tomato leaves

Endophytic fungi	No. of records	Frequency (%)
<i>Alternaria alternata</i> (Fr) Keissl	5	10
<i>Aspergillus terrus</i> (Thom)	4	8
<i>Chaetomium globosum</i> Kunze	3	6
<i>Cladosporium cladosporioides</i> (Fresen.) G. A. de vries	5	10
<i>Cladosporium herbarum</i> Pers.	1	2
<i>Epicoccum nigrum</i> Link	15	30
<i>Fusarium oxysporum</i> Schltdl.	2	4
Morphotaxon 1	2	4
Morphotaxon 2	1	2
Morphotaxon 3	1	2
Morphotaxon 4	3	6
<i>Trichoderma harzianum</i> Rifai	3	6

*E. nigrum* is considered one of the most important fungal species that produce bioactive secondary metabolites [43,44], which why we decided to focus our work on this fungus species. *E. nigrum* morphology characterized by vigorous aerial mycelial growth, irregular margins, intense

orange color and orange to dark red color reverse in PDA and malt media (Fig. 1A). Conidia are globose pyriform in shape, formed singly on densely, mostly 15-25  $\mu\text{m}$  diameter with a funnel-shaped base and broad attachment scar with slightly pigmented conidiophores (Fig. 1B). All these morphological observations supported the notion that this isolated fungus corresponded to *Epicoccum nigrum*. The genomic DNA of the fungal isolate was purified, amplified, sequenced and deposited in GenBank under accession number KR023621. Alignment with *Epicoccum nigrum* rDNA in NCBI GenBank (GU934519) resulted in a 100% identity match. The phylogenetic tree was constructed for *E. nigrum* ASU1 isolate from multiple sequence alignment of 18S rDNA gene sequences (Fig. 1C).

### 3.2 Curvularin as an extracellular product of *Epicoccum nigrum* ASU1

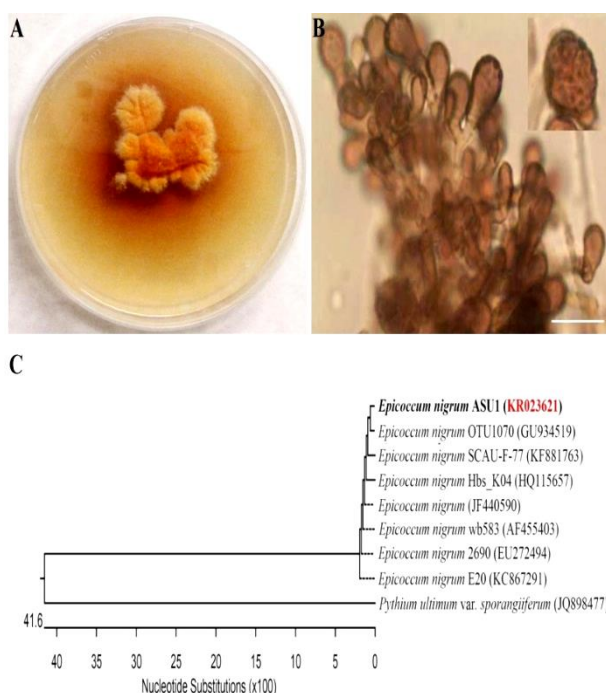


**Figure 1:** *Epicoccum nigrum* ASU1. (A) 10 days old culture at 25°C on PDA medium; (B) Microscopic features showing conidia and conidiophores (Scale bar = 10 $\mu\text{m}$ ); (C) Phylogenetic tree of *Epicoccum nigrum* ASU1 with reference strains. Numbers at the respective nodes are percentage of 1000 bootstrap replicates. Bar indicates genetic distance due to sequence variation.

In this investigation, we decided to analyze the potential of our particular *Epicoccum nigrum* ASU1 isolate to produce interesting bioactive secondary metabolites. The antioxidant compound curvularin was purified for the first time from the ethyl acetate extract of *E. nigrum* ASU1 partitioned between n-hexane and 90% aqueous methanol. The MS spectra showed molecular ion peaks at  $m/z$  293.2  $[\text{M}+\text{H}]^+$  (base peak) and  $m/z$  291.5  $[\text{M}-\text{H}]^-$  (base peak), respectively, indicating a molecular weight of 292 g/mol

(Fig. 2A).

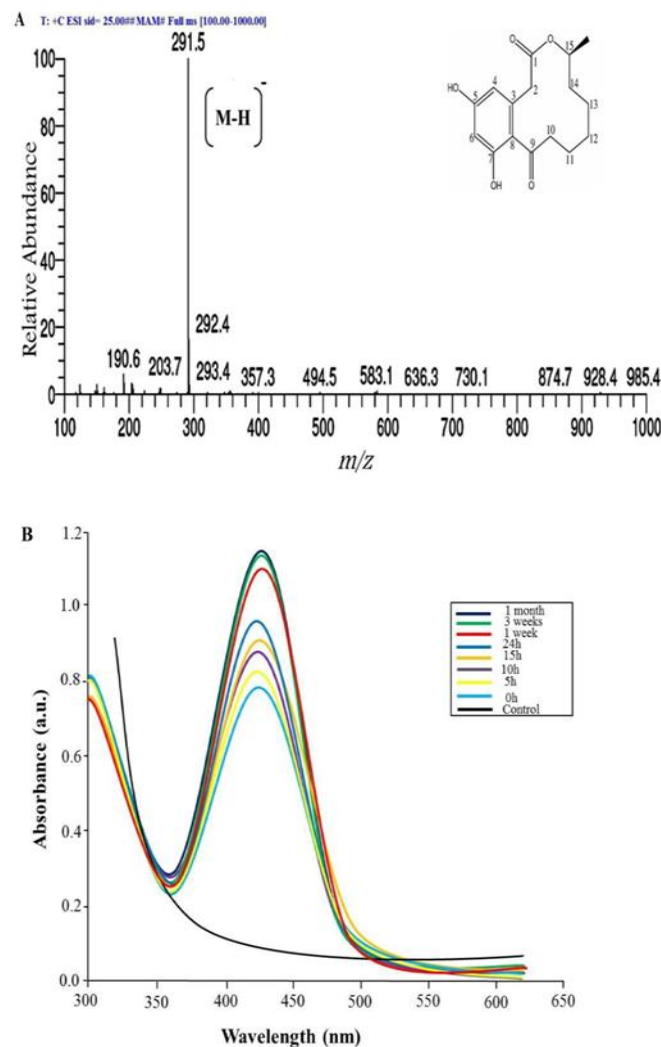


**Figure 2:** Curvularin and biosynthesis of AgNPs. (A) Mass spectra of the compound curvularin; (B) Synthesis of AgNPs using compound curvularin: UV spectra of synthesized AgNPs at different time intervals.

Additionally, the MS spectra showed the presence of the characteristic ion with  $m/z$  203 which indicate that the carbonyl function at C-9 was conjugated to the aromatic ring [45]. The UV absorbance of curvularin was at  $\lambda_{\text{max}}$  (methanol) 202.5, 222.0, 271.9 and 298.9 nm indicating that it had a 2,4-dihydroxyacetophenone chromophore. The  $^1\text{H}$  NMR and  $^{13}\text{C}$  spectra (Table 2) showed a pair of *meta*-coupled aromatic protons at  $\alpha\text{H}$  6.24 (H-6) and 6.21 (H-4), respectively. In addition, the spectrum contained a diastereotopic methylene function resonating at  $\alpha\text{H}$  3.85 and 3.61 ( $\text{CH}_2$ - 2) as well as an extended aliphatic spin system which could only be completely assembled with help of the COSY spectrum due to a significant degree of overlapping. There is a long range coupling between H-4 and  $\text{CH}_2$ -2 according to COSY spectrum and also there is a correlation between  $\text{CH}_2$ -2 and C-3, C-4, C-8, and the ester

carbonyl at  $\delta$ C 173.0 (C-1), the oxygen atom of which had to be connected to H-15 which all appeared in HMBC spectrum. The UV spectra, MS,  $^1\text{H}$  and  $^{13}\text{C}$  NMR spectra exhibited that the isolated compound has sixteen carbon atoms with molecular formula  $\text{C}_{16}\text{H}_{20}\text{O}_5$ . As a result, the isolated compound was identified as curvularin, by comparing the obtained data of UV, MS  $^1\text{H}$  and  $^{13}\text{C}$  NMR data with reference published papers [46,47].

**Table 2:**  $^1\text{H}$ ,  $^{13}\text{C}$  NMR, COSY and HMBC data of isolated compound at 500 ( $^1\text{H}$ ) and 125 ( $^{13}\text{C}$ ) MHz

Nr	$^1\text{H}$ (MeOD)	COSY	HMBC	$^{13}\text{C}$ (MeOD)
1				173.0
2A	3.85, d (15.7)	2B,4	1,3,4,8	40.6
2B	3.61, d (15.7)	2A,4	1,3,4,8	
3				137.5
4	6.21, d (2.2)	2A/B, 6	2,6,8	112.6
5				161.5
6	6.24, d (2.2)	4	4,5,8	102.9
7				
8				121.0
9				
10	A 3.20, ddd (15.2, 8.8, 2.8) B 2.73, ddd (15.2, 9.7, 2.8)	10B, 11A/B 10A, 11A/B		
11	A 1.74, m B 1.57, m	10A/B, 11B, 12A/B 10A/B, 11A, 12A/B		
12A	1.39, m	11A/B, 12B, 13A/B		
12B	1.26, m	11A/B, 12A, 13A/B		
13A	1.47, m	12A/B, 13B, 14A/B		
13B	1.30, m	12A/B, 13A, 14A/B		
14A	1.59, m	13A/B, 14B, 15		33.0
14B	1.43, m	13A/B, 14A, 15		
15	4.92, m	CH3, 14A/B		73.9
CH <sub>3</sub>	1.12, d (6.3)	15	14,15	20.5

### 3.3 Biosynthesis and characterization of AgNPs

We went on to assay the possibility of biosynthesizing AgNPs using the curvularin compound obtained from the *Epicoccum nigrum* ASU1. The formation of AgNPs was firstly evaluated visually by observing the colour change of the  $\text{AgNO}_3$  solution after challenging with 2 mL of curvularin. The UV-vis absorption spectrum showed a strong absorption peak centered at 430 nm at different time intervals, which is characteristic of surface plasmon resonance of silver, and hence indicated the formation of AgNPs (Fig. 2B). Moreover, the increase in the absorbance of AgNPs was easily observed with a prolonged reaction time, which indicated a greater reduction of  $\text{Ag}^+$  ions and the formation of more AgNPs. The UV-vis absorption spectra also showed good stability of the formed AgNPs after being stored for one month at room temperature which are well dispersed in solution without any aggregation (Fig. 2B).

#### 3.3.1 Characterization of biosynthesized AgNPs

The size and morphology of the biosynthesized AgNPs were examined by HR-TEM. Images showed the formation of spherical shaped and polydispersive structures with an

average particle size of  $37 \pm 1.2$  nm (Fig. 3A, B). DLS measurements of AgNPs showed that the hydrodynamic average of AgNPs size and Zeta potential were found to be around 40 nm and -16mV, respectively (Fig. 3 C, D). PDI of 0.25 indicates the good mono-dispersity and -ve zeta potential indicates good stability with capping by negatively charged groups of nanoparticles. The DLS data are in agreement with that of TEM analysis. The slightly differences between TEM and DLS measurements are possibly and may be backed to the drying forces present during preparation the TEM samples. Moreover, DLS analysis investigates the hydrodynamic diameter of the particles in solution which is based on the Brownian motion of the particles itself in the solvent which used. Moreover, the hydrodynamic diameter of a particle in a specific solvent is dependent on different factors including the temperature, viscosity, and the translational diffusion coefficient of the particles. However, the hydrodynamic diameter measures all molecular size included in the stabilizer and hydration layer of water molecules.

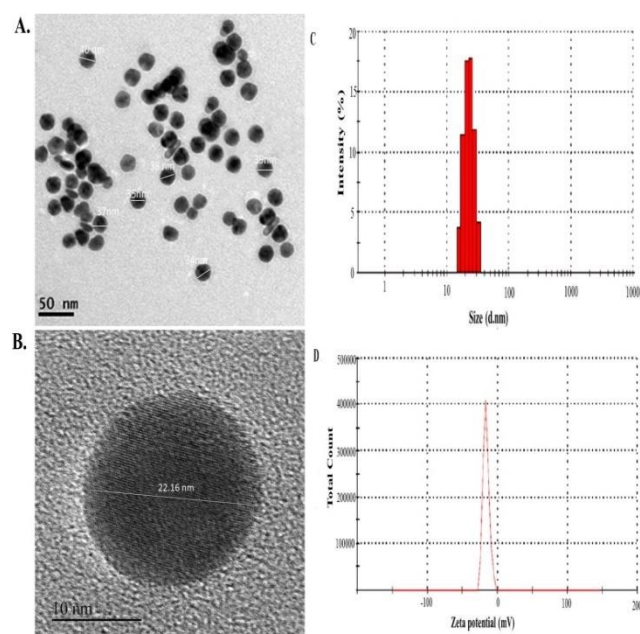


**Figure 3:** Characterization of biosynthesized AgNPs by TEM and DLS. (A) General HR-TEM images of well-dispersed AgNPs; (B) Well-spherical shaped AgNP. Size is indicated; Particle size distribution. (C) Dynamic light scattering measurements (DLS); (D) Zeta potential of AgNPs

The SAED pattern showed circular rings, which can be indexed in accordance with the reflections from the (111), (200), (220) and (311) planes (JCPDS 04-0783). These planes corresponded to face-centered cubic (fcc) Ag and revealed the polycrystalline nature of the biosynthesized AgNPs (Fig. 4A). The EDX spectrum showed a strong typical optical absorption peak at approximately 3 keV,

which was attributed to the SPR of the metallic Ag nanoparticles and confirmed the significant presence of pure metallic Ag with no other elemental contaminants. The EDX spectrum also showed other bands for carbon (C) and oxygen (O) peaks besides the Ag peak (Fig. 4B), apparently due to the scattering caused by the capping agent. This observation supports the notion that the curvularin compound acts as a stabilizing agent of AgNPs.

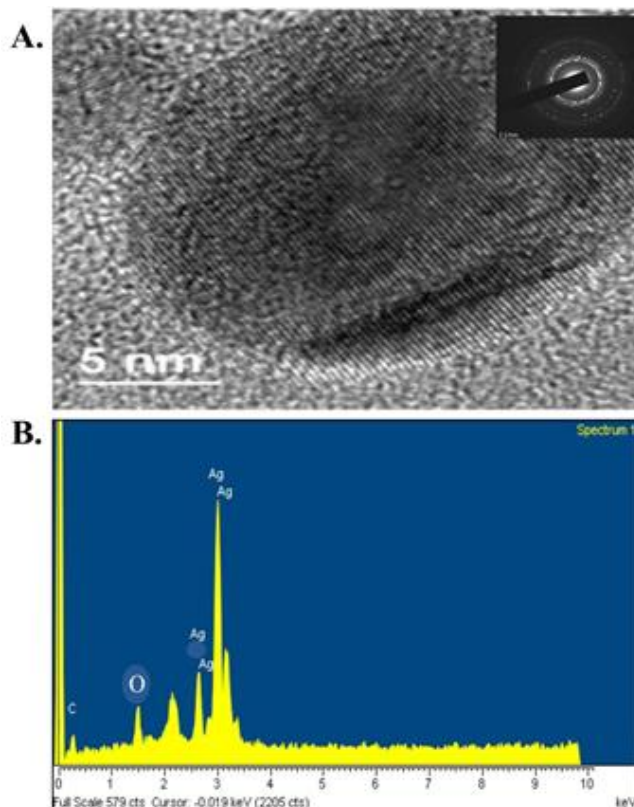


**Figure 4:** Characterization of AgNPs. (A) SAED analysis. (B) EDX spectrum displaying the purity of the AgNPs

The crystalline nature of AgNPs was further confirmed by the XRD analysis, whereas the XRD pattern revealed the typical fcc structure of AgNPs [40]. The XRD spectrum showed four main characteristic Bragg diffraction peaks at  $2\theta$  values of nearly  $38.68^\circ$ ,  $46.1^\circ$ ,  $64.11^\circ$  and  $77.4^\circ$  which respectively corresponded to the (111), (200), (220), and (311) planes of fcc Ag (Fig. 5A-B). The diffraction peaks were consistent with standard database files (JCPDS card No. 04-0783), which indicate that the synthesized nanoparticles were pure crystalline in nature, and this finding is in accordance with the SAED results. FTIR measurements were carried out to identify the possible functional groups in curvularin responsible for the reduction of the  $\text{Ag}^+$  ions, capping and efficient stabilization of the biosynthesized AgNPs (Fig. 5C). The FTIR spectrum of curvularin showed bands at  $3304\text{ cm}^{-1}$  for  $-\text{OH}$  stretching (aliphatic hydroxyl group),  $2928\text{ cm}^{-1}$  for  $\text{C}-\text{H}$  stretching (aliphatic  $\text{C}-\text{H}$ ), and  $1639\text{ cm}^{-1}$  for carbonyl stretching ( $\text{C}=\text{O}$ , carbonyl group) (Fig. 5C). There is deviation of both hydroxyl and carbonyl group, whereas it

appears at  $3338$  and  $1636\text{ cm}^{-1}$ , indicating that these groups are better able to bind metal and can possibly form metal nanoparticles (i.e. capping AgNPs) to prevent agglomeration and to, therefore, stabilize the medium.

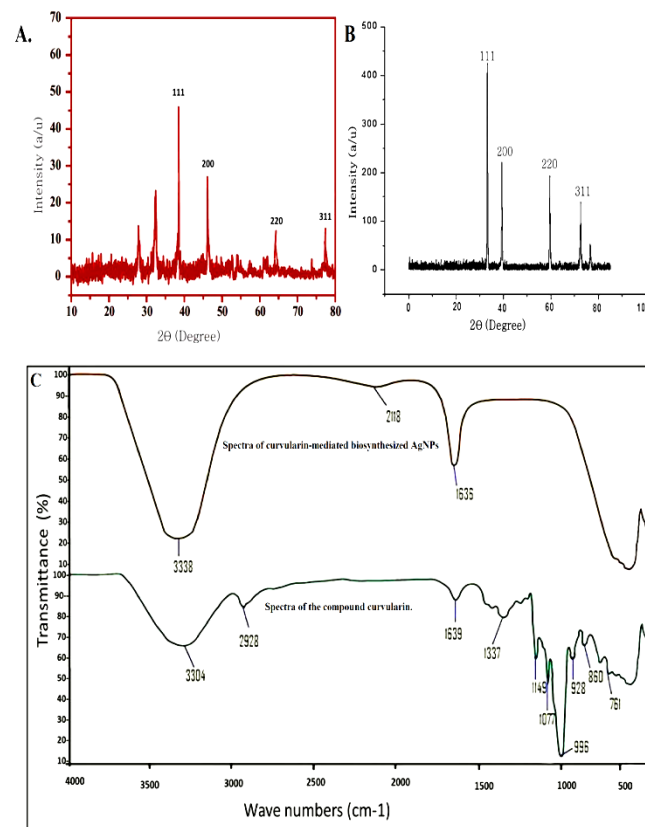


**Figure 5 :** X-ray diffraction patterns AgNPs. (A) XRD of AgNPs (B) XRD of Ag; (C) FTIR spectra of the compound curvularin and curvularin-mediated biosynthesized AgNPs.

### 3.4 Antifungal activity of the biosynthesized AgNPs

Finally, the antifungal activity of both the compound curvularin and the AgNPs capped curvularin was assayed. Three different concentrations (5, 10 and 20 ppm) from each were analysed in PDA plates against the pathogenic fungus *Alternaria solani*, the causal agent of tomato early blight disease. The results clearly showed that all tested concentrations for the both inhibited the mycelial growth of *Alternaria solani* to various extents (Fig. 6). Interestingly, the results also indicated the great antifungal activity of AgNPs capped curvularin compared to curvularin alone (Fig. 6). Biosynthesized AgNPs with concentrations 5, 10 and 20 ppm showed mycelial reductions comprising 55.6, 91.1 and 95.6%, respectively. On the other hand, curvularin caused mycelia reduction contributing 16.7, 33.3 and 44.4%, respectively (Fig. 6). Those findings indicated the high potential activity of AgNPs as antifungal agents against phytopathogenic fungi at lowest concentrations which can be used as better alternatives to synthetic fungicides.

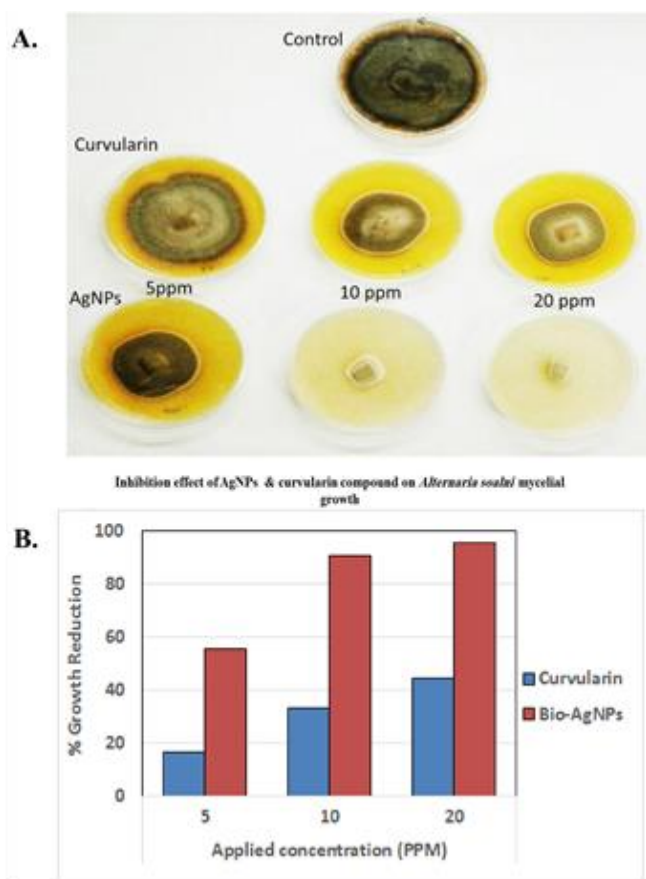


**Figure 6:** Inhibitory effect of compound curvularin and AgNPs capped curvularin against *Alternaria solani*: (A) Culture growth at 8 days; (B) % mycelial growth reduction of *Alternaria solani*.

#### 4 Discussion

In this study, *Epicoccum nigrum* was isolated and identified as a prevalent endophytic fungus (30% frequency) associated with healthy tomato leaves. Endophytic fungi are those living in the interior of apparently healthy and asymptomatic plant hosts. Fungi fitting this description appear to be ubiquitous. Indeed, no study has yet shown the existence of a plant species without endophytes [48]. In this respect, many investigations emphasized that *Epicoccum nigrum* was frequently isolated as endophyte from many crops [49,50]. Endophytic fungus *E. nigrum* is considered one of the most important fungal species that produce bioactive secondary metabolites [43,44]. Beside the traditional identification of *Epicoccum nigrum* ASU1, it was identified at molecular level and deposited in GenBank under accession number KR023621.

*Epicoccum nigrum* was a source of natural compounds with biological properties including antioxidants, anti-thrombosis, antihypertensive, antifibrosis, and antiviral activities [43,51,52]. Therefore, we decided to evaluate the potential of *E. nigrum* ASU1 to produce interesting bioactive secondary metabolites.

In this investigation, the antioxidant compound curvularin was purified for the first time from the ethyl acetate extract of *E. nigrum* ASU1. The UV spectra, MS,  $^1\text{H}$  and  $^{13}\text{C}$  NMR spectra exhibited that the isolated compound has sixteen carbon atoms with molecular formula  $\text{C}_{16}\text{H}_{20}\text{O}_5$ . As a result, the isolated compound was identified as curvularin, by comparing the obtained data of UV, MS  $^1\text{H}$  and  $^{13}\text{C}$  NMR data with reference data [45,53]. In this respect, curvularin compound has been previously reported as an extracellular metabolite produced by many fungal genera such as *Curvularia* [54,46], *Alternaria* ([47] and *Penicillium* [55,56].

The biosynthesis process of AgNPs using curvularin compound was firstly evaluated visually by observing the color change to reddish brown and dark-brown due to the excitation of the surface plasmon resonance (SPR) effect. This observation was in agreement with the procedures of preparation of metal nanoparticles [57].

The UV-Vis spectrum showed a strong absorbance peak centered at 425 nm at different time intervals which is characteristic for surface plasmon resonance of silver [58] and hence indicate the formation of AgNPs. The UV-vis absorption spectra also showed good stability of the formed AgNPs after being stored for one month at room temperature which are well dispersed in solution without any aggregation. Additionally, the AgNPs capped curvularin were characterized by Fourier transform infrared (FT-IR) spectroscopy, X-ray diffraction (XRD), selected area electron diffraction (SAED), energy dispersive X-ray spectroscopy (EDX), and high-resolution transmission electron microscopy (HR-TEM). The results showed the formation of high purified spherical AgNPs with an average size of 37 nm. The FT-IR results suggested that both hydroxyl and carbonyl functional groups in curvularin are responsible for the reduction of the  $\text{Ag}^+$  ions and stabilizing AgNPs.

Moreover, this study recommends that curvularin compound, purified from the fungal culture, may play two roles in the biosynthesis and stabilization of AgNPs in the aqueous medium. This study suggests acceptable mechanism of AgNPs synthesis using the compound curvularin according to the presence of hydroxyl and carbonyl groups in curvularin compound. During reduction process, the hydroxyl groups were likely oxidized to carbonyl groups and silver ions were reduced through free electron produced to form AgNPs. An intermediate silver complex was formed and finally silver ions and dehydrocurvularin compound were formed. The possible capping mechanism of silver nanoparticles, whereas the interaction of hydroxyl and carbonyl groups of curvularin compound with AgNPs has been shown. In this respect, Sun *et al.* [59] confirm the ability of silver to build eight hydrogen bonds with many ligands.

The antifungal activity of both the compound curvularin and the AgNPs capped curvularin was analysed using three

different concentrations (5, 10 and 20 ppm) against the pathogenic fungus *Alternaria solani*, the causal agent of tomato early blight disease. The results proved that curvularin and AgNPs capped curvularin, all tested concentrations, inhibited the mycelial growth of *A. solani*. Interestingly, AgNPs capped curvularin showed antifungal activity greater than using curvularin alone. Those findings indicated the high potential activity of AgNPs as antifungal agents against phytopathogenic fungi at lowest concentrations which can be used as better alternatives to synthetic fungicides. Several studies reported the inhibitory mode of action of AgNPs against microbes [42,60], however, the exact mechanism of their antimicrobial potential is not fully understood [61]. More precisely, a number of works have suggested that for their ability to form free radicals that could interact with the microbe membrane lipids and then disturb and finally spoil their functions [62]. Others owed that to their ability to disrupt the fungal transport systems through ion efflux [63]. The dysfunction of ion efflux can cause rapid accumulation of  $\text{Ag}^+$  ions, which interrupts cellular processes such as metabolism and respiration by reacting with molecules. Stoimenov et al. [63] have depicted a new finding; the membrane could be deteriorated by the formation of pits on the surface of the cell wall membrane of microorganisms. This leads to increase the cell permeability and to disturb the ion transport in cell system that results in the final cell death [61,64]. So, the green-synthesized AgNPs is a good unique route, which is easily produced and can extensively useful in plant disease management.

## 5 Conclusion

In conclusion, we have herein reported a facile and rapid approach for green synthesis of AgNPs using the compound curvularin extracted from cultural filtrates of *Epicoccum nigrum* ASU1. The compound curvularin was used as both a reducing agent and stabiliser in the AgNPs synthesis at ambient conditions without additional any external reagents. The formed AgNPs are spherical in shape with an average size around  $37 \pm 1.2$  nm diameters at different time intervals, suggesting that they are also stable in aqueous solution. Both carbonyl and hydroxyl groups of compound curvularin have strong binding affinity to silver, suggesting the formation of a thin layer covering the formed AgNPs acting as a stabilising agent and also to prevent their agglomeration. Moreover, our data demonstrated that the AgNPs capped curvularin have potent antifungal activity at lowest concentrations compared to curvularin alone against the phytopathogenic fungus *Alternaria solani*. Taken together; this suggests that the AgNPs capped curvularin, synthesized via the one-step reduction method will explore their competence in plant protection field for the control of various phytopathogenic fungi. Undoubtedly, further research is needed in this area to explore other possible biomolecule derived fungi acting as reducing/capping agents in the synthesis of different nanomaterials with various biological activities without the need to use such

expensive chemical and physical methods. Furthermore, with the recent progress and the ongoing efforts in improving nanomaterials synthesis efficiency and exploring their antimicrobial applications, it is hopeful that the execution of the approach of ours on a large scale and their commercial applications in plant disease management will be very much useful in the upcoming years.

## Acknowledgment

A financial support from European Commission by Erasmus Mundus Scholarship-ACTION 2 WELCOME programme is gratefully acknowledged. Work in JAD laboratory was supported by grant BIO2014-54269-R from the Ministerio de Economía y Competividad (Spain). We are also immensely grateful to Professor/ Mohamed Ismail (Department of analytical chemistry, Sohag University, Egypt) for his critical reading of the chemical analysis of curvularin.

**Conflict of Interest:** The authors declare no conflict of interest and no competing financial interests.

## References

- [1] Simi C, Abraham TE (2007) Hydrophobic grafted and cross-linked starch nanoparticles for drug delivery. *Bioprocess Biosyst Eng* 30 (3):173-180. doi: [10.1007/s00449-007-0112-5](https://doi.org/10.1007/s00449-007-0112-5)
- [2] Bhattacharya R, Mukherjee P (2008) Biological properties of "naked" metal nanoparticles. *Adv Drug Deliv Rev* 60 (11):1289-1306. doi: [10.1016/j.addr.2008.03.013](https://doi.org/10.1016/j.addr.2008.03.013)
- [3] Kathiravan V, Ravi S, Ashokkumar S, Velmurugan S, Elumalai K, Khatiwada CP (2015) Green synthesis of silver nanoparticles using *Croton sparsiflorus morong* leaf extract and their antibacterial and antifungal activities. *Spectrochimica Acta Part A: Mol Biomol Spectrosc* 139:200-205. doi: [10.1016/j.saa.2014.12.022](https://doi.org/10.1016/j.saa.2014.12.022)
- [4] Abbaspour A, Norouz-Sarvestani F, Noori A, Soltani N (2015) Aptamer-conjugated silver nanoparticles for electrochemical dual-aptamer-based sandwich detection of *Staphylococcus aureus*. *Biosens Bioelectron* 68:149-155. doi: [10.1016/j.bios.2014.12.040](https://doi.org/10.1016/j.bios.2014.12.040)
- [5] Sharma VK, Yngard RA, Lin Y (2009) Silver nanoparticles: green synthesis and their antimicrobial activities. *Adv Colloid Interface Sci* 145 (1):83-96. doi: [10.1016/j.cis.2008.09.002](https://doi.org/10.1016/j.cis.2008.09.002)
- [6] Schultz S, Smith DR, Mock JJ, Schultz DA (2000) Single-target molecule detection with nonbleaching multicolor optical immunolabels. *Proc Nat Acad Sci* 97 (3):996-1001
- [7] Eckhardt S, Brunetto PS, Gagnon J, Priebe M, Giese B, Fromm KM (2013) Nanobio silver: its interactions with peptides and bacteria, and its uses in medicine. *Chem Rev* 113 (7):4708-4754. doi: [10.1021/cr300288v](https://doi.org/10.1021/cr300288v)
- [8] Kumar B, Smita K, Cumbal L, Debut A (2014) Biogenic synthesis of iron oxide nanoparticles for 2-arylbenzimidazole fabrication. *J Saudi Chem Soc* 18 (4):364-369. doi: [10.1016/j.jscs.2014.01.003](https://doi.org/10.1016/j.jscs.2014.01.003)
- [9] Gittins DI, Bethell D, Nichols RJ, Schiffrin DJ (2000) Diode-like electron transfer across nanostructured films containing a

- redox ligand. *J Mater Chem* 10 (1):79-83. doi: [10.1039/a902960e](https://doi.org/10.1039/a902960e)
- [10] Jaworska A, Malek K (2014) A comparison between adsorption mechanism of tricyclic antidepressants on silver nanoparticles and binding modes on receptors. Surface-enhanced Raman spectroscopy studies. *J Colloid Interface Sci* 431:117-124. doi:[10.1016/j.jcis.2014.05.060](https://doi.org/10.1016/j.jcis.2014.05.060)
- [11] Warriner K, Reddy SM, Namvar A, Neethirajan S (2014) Developments in nanoparticles for use in biosensors to assess food safety and quality. *Trends Food Sci Technol* 40 (2):183-199. doi: [10.1016/j.tifs.2014.07.008](https://doi.org/10.1016/j.tifs.2014.07.008)
- [12] Ko J, Lee C, Choo J (2015) Highly sensitive SERS-based immunoassay of aflatoxin B1 using silica-encapsulated hollow gold nanoparticles. *J Hazard Mater* 285:11-17. doi: [10.1016/j.jhazmat.2014.11.018](https://doi.org/10.1016/j.jhazmat.2014.11.018)
- [13] Narayanan KB, Sakthivel N (2010) Biological synthesis of metal nanoparticles by microbes. *Adv Colloid Interface Sci* 156 (1):1-13. doi: [10.1016/j.cis.2010.02.001](https://doi.org/10.1016/j.cis.2010.02.001)
- [14] Das J, Velusamy P (2014) Catalytic reduction of methylene blue using biogenic gold nanoparticles from *Sesbania grandiflora* L. *J Taiwan Inst Chem Eng* 45 (5):2280-2285. doi: [10.1016/j.jtice.2014.04.005](https://doi.org/10.1016/j.jtice.2014.04.005)
- [15] Cao X, Cheng C, Ma Y, Zhao C (2010) Preparation of silver nanoparticles with antimicrobial activities and the researches of their biocompatibilities. *J Mater Sci Mater Med* 21 (10):2861-2868. doi: [10.1007/s10856-010-4133-2](https://doi.org/10.1007/s10856-010-4133-2)
- [16] Flores CY, Miñán AG, Grillo CA, Salvarezza RC, Vericat C, Schilardi PL (2013) Citrate-Capped Silver Nanoparticles Showing Good Bactericidal Effect against Both Planktonic and Sessile Bacteria and a Low Cytotoxicity to Osteoblastic Cells. *ACS Appl Mater Interfaces* 5 (8):3149-3159. doi: [10.1021/am400044e](https://doi.org/10.1021/am400044e)
- [17] Pingali KC, Rockstraw DA, Deng S (2005) Silver nanoparticles from ultrasonic spray pyrolysis of aqueous silver nitrate. *Aerosol Sci Technol* 39 (10):1010-1014. doi: [10.1080/02786820500380255](https://doi.org/10.1080/02786820500380255)
- [18] Wang X, Zuo J, Keil P, Grundmeier G (2007) Comparing the growth of PVD silver nanoparticles on ultra thin fluorocarbon plasma polymer films and self-assembled fluoroalkyl silane monolayers. *Nanotechnol* 18 (26):265303. doi: [10.1088/0957-4484/18/26/265303](https://doi.org/10.1088/0957-4484/18/26/265303)
- [19] Shin HS, Yang HJ, Kim SB, Lee MS (2004) Mechanism of growth of colloidal silver nanoparticles stabilized by polyvinyl pyrrolidone in  $\gamma$ -irradiated silver nitrate solution. *J Colloid Interface Sci* 274 (1):89-94. doi: [10.1016/j.jcis.2004.02.084](https://doi.org/10.1016/j.jcis.2004.02.084)
- [20] Huang J, Zhan G, Zheng B, Sun D, Lu F, Lin Y, Chen H, Zheng Z, Zheng Y, Li Q (2011) Biogenic silver nanoparticles by *Cacumen platycladi* extract: synthesis, formation mechanism, and antibacterial activity. *Ind Eng Chem Res* 50 (15):9095-9106. doi: [10.1021/ie200858y](https://doi.org/10.1021/ie200858y)
- [21] Kumar B, Smita K, Cumbal L, Debut A (2014) Sacha inchi (*Plukenetia volubilis* L.) shell biomass for synthesis of silver nanocatalyst. *J Saudi Chem Soci.* doi: [10.1016/j.jscs.2014.03.005](https://doi.org/10.1016/j.jscs.2014.03.005)
- [22] Kumar B, Smita K, Cumbal L, Debut A, Pathak RN (2014) Sonochemical synthesis of silver nanoparticles using starch: a comparison. *Bioinorg Chem Appl.* doi: [10.1155/2014/784268](https://doi.org/10.1155/2014/784268)
- [23] Ahmed KBA, Kalla D, Uppuluri KB, Anbazhagan V (2014) Green synthesis of silver and gold nanoparticles employing levan, a biopolymer from *Acetobacter xylinum* NCIM 2526, as a reducing agent and capping agent. *Carbohydr Polym* 112:539-545. doi: [10.1016/j.carbpol.2014.06.033](https://doi.org/10.1016/j.carbpol.2014.06.033)
- [24] Qian Y, Yu H, He D, Yang H, Wang W, Wan X, Wang L (2013) Biosynthesis of silver nanoparticles by the endophytic fungus *Epicoccum nigrum* and their activity against pathogenic fungi. *Bioprocess Biosyst Eng* 36 (11):1613-1619. doi: [10.1007/s00449-013-0937-z](https://doi.org/10.1007/s00449-013-0937-z)
- [25] Bhattacharya D, Gupta RK (2005) Nanotechnology and potential of microorganisms. *Crit Rev Biotechnol* 25 (4):199-204. doi: [10.1080/07388550500361994](https://doi.org/10.1080/07388550500361994)
- [26] Abdel-Hafez SI, Nafady NA, Abdel-Rahim IR, Shaltout AM, Mohamed MA (2016) Biogenesis and Optimisation of Silver Nanoparticles by the Endophytic Fungus *Cladosporium sphaerospermum*. *Int J Nanomater Chem* 2 (1):11-19. doi: [10.18576/ijnc/020103](https://doi.org/10.18576/ijnc/020103)
- [27] Dadosh T (2009) Synthesis of uniform silver nanoparticles with a controllable size. *Mater Lett* 63 (26):2236-2238. doi: [10.1016/j.matlet.2009.07.042](https://doi.org/10.1016/j.matlet.2009.07.042)
- [28] Tanvir S, Oudet F, Pulvin S, Anderson WA (2012) Coenzyme based synthesis of silver nanocrystals. *Enzyme Microb Technol* 51 (4):231-236. doi: [10.1016/j.enzmictec.2012.07.002](https://doi.org/10.1016/j.enzmictec.2012.07.002)
- [29] Liu L, Yang J, Xie J, Luo Z, Jiang J, Yang YY, Liu S (2013) The potent antimicrobial properties of cell penetrating peptide-conjugated silver nanoparticles with excellent selectivity for Gram-positive bacteria over erythrocytes. *Nanoscale* 5 (9):3834-3840. doi: [10.1039/c3nr34254a](https://doi.org/10.1039/c3nr34254a)
- [30] Ghodake G, Lim S-R, Lee DS (2013) Casein hydrolytic peptides mediated green synthesis of antibacterial silver nanoparticles. *Colloids Surf B: Biointerfaces* 108:147-151. doi: [10.1016/j.colsurfb.2013.02.044](https://doi.org/10.1016/j.colsurfb.2013.02.044)
- [31] Mohamed MA (2015) One-step functionalization of silver nanoparticles using the orsellinic acid compound isolated from the endophytic fungus *Epicoccum nigrum*: characterization and antifungal activity. *Int J Nanomater Chem* 1 (3):103-110
- [32] Dipankar C, Murugan S (2012) The green synthesis, characterization and evaluation of the biological activities of silver nanoparticles synthesized from *Iresine herbstii* leaf aqueous extracts. *Colloids Surf B: Biointerfaces* 98:112-119. doi: [10.1016/j.colsurfb.2012.04.006](https://doi.org/10.1016/j.colsurfb.2012.04.006)
- [33] Verma VC, Kharwar RN, Gange AC (2010) Biosynthesis of antimicrobial silver nanoparticles by the endophytic fungus *Aspergillus clavatus*. *Nanomed* 5 (1):33-40. doi: [10.2217/nnm.09.77](https://doi.org/10.2217/nnm.09.77)
- [34] Smith NR, Dawson VT (1944) The bacteriostatic action of rose bengal in media used for plate counts of soil fungi. *Soil Sci* 58 (6):467-472. doi: [10.1097/00010694-194412000-00006](https://doi.org/10.1097/00010694-194412000-00006)
- [35] Abdel-Hafez SI, Abo-Elyousr kA, Abdel-Rahim IR (2015) Leaf surface and endophytic fungi associated with onion leaves and their antagonistic activity against *Alternaria porri*. *Czech Mycol* 67 (1):1-22
- [36] Sinclair JB, Dhingra OD (1995) *Basic Plant Pathology Methods*. CRC Press, Boca Raton, Florida, USA.

- [37] Ellis B (1971) Dematiaceous Hyphomycetes. vol no. 125. CMI, Kew, Surrey, England.
- [38] Domsch KKH, Gams W, Anderson TH (1980) Compendium of Soil Fungi. vol v. 1. Academic Press, London
- [39] Gardes M, Bruns TD (1993) ITS primers with enhanced specificity for basidiomycetes-application to the identification of mycorrhizae and rusts. Mol Ecol 2 (2):113-118. doi: [10.1111/j.1365-294x.1993.tb00005.x](https://doi.org/10.1111/j.1365-294x.1993.tb00005.x)
- [40] Cullity B (1978) Elements of XRD. USA Edison-Wesley P Inc
- [41] Siddique YH, Fatima A, Jyoti S, Naz F, Khan W, Singh BR, Naqvi AH (2013) Evaluation of the toxic potential of graphene copper nanocomposite (GCNC) in the third instar larvae of transgenic *Drosophila melanogaster* (hsp70-lacZ) Bg9. PloS one 8 (12):e80944. doi: [10.1371/journal.pone.0080944](https://doi.org/10.1371/journal.pone.0080944)
- [42] Kim SW, Jung JH, Lamsal K, Kim YS, Min JS, Lee YS (2012) Antifungal effects of silver nanoparticles (AgNPs) against various plant pathogenic fungi. Mycobiol 40 (1):53-58. doi: [10.5941/myco.2012.40.1.053](https://doi.org/10.5941/myco.2012.40.1.053)
- [43] Wang J-M, Ding G-Z, Fang L, Dai J-G, Yu S-S, Wang Y-H, Chen X-G, Ma S-G, Qu J, Xu S (2010) Thiodiketopiperazines produced by the endophytic fungus *Epicoccum nigrum*. J Nat Prod 73 (7):1240-1249. doi: [10.1021/np1000895](https://doi.org/10.1021/np1000895)
- [44] Musetti R, Grisan S, Polizzotto R, Martini M, Paduano C, Osler R (2011) Interactions between 'Candidatus Phytoplasma mali' and the apple endophyte *Epicoccum nigrum* in *Catharanthus roseus* plants. J Appl Microbiol 110 (3):746-756. doi: [10.1111/j.1365-2672.2011.04937.x](https://doi.org/10.1111/j.1365-2672.2011.04937.x)
- [45] Munro H, Musgrave O, Templeton R (1967) Curvularin. Part V. The compound C<sub>16</sub> H<sub>18</sub> O<sub>5</sub>, αβ-dehydrocurvularin. J Chem Soc C: Organic:947-948. doi: [10.1039/j39670000947](https://doi.org/10.1039/j39670000947)
- [46] Musgrave O (1956) Curvularin. Part I. Isolation and partial characterisation of a metabolic product from a new species of *Curvularia*. J Chem Soc 4301-4305. doi: [10.1039/jr9560004301](https://doi.org/10.1039/jr9560004301)
- [47] Robeson D, Strobel G (1981) Alpha, beta-dehydrocurvularin and curvularin from *Alternaria cinerariae*. Zeitschrift fur Naturforschung C Biosci 36:1081 -1083
- [48] Promptutha I, Lumyong S, Dhanasekaran V, McKenzie EHC, Hyde KD, Jeewon R (2007) A phylogenetic evaluation of whether endophytes become saprotrophs at host senescence. Microb Ecol 53 (4):579-590. doi: [10.1007/s00248-006-9117-x](https://doi.org/10.1007/s00248-006-9117-x)
- [49] Martini M, Musetti R, Grisan S, Polizzotto R, Borselli S, Pavan F, Osler R (2009) DNA-dependent detection of the grapevine fungal endophytes *Aureobasidium pullulans* and *Epicoccum nigrum*. Plant Dis 93 (10):993-998. doi: [10.1094/pdis-93-10-0993](https://doi.org/10.1094/pdis-93-10-0993)
- [50] Favaro LC, dL, de Souza Sebastianes FL, Araujo WL (2012) *Epicoccum nigrum* P16, a sugarcane endophyte, produces antifungal compounds and induces root growth. PloS one 7 (6):e36826. doi: [10.1371/journal.pone.0036826](https://doi.org/10.1371/journal.pone.0036826)
- [51] Zhang Y, Liu S, Che Y, Liu X (2007) Epicoccins A–D, epipolythiodioxopiperazines from a *Cordyceps*-colonizing isolate of *Epicoccum nigrum*. J Nat Prod 70 (9):1522-1525. doi: [10.1021/np070239u](https://doi.org/10.1021/np070239u)
- [52] Madrigal C, Tadeo J, Melgarejo P (1991) Relationship between flavipin production by *Epicoccum nigrum* and antagonism against *Monilinia laxa*. Mycol Res 95 (12):1375-1381. doi: [10.1016/s0953-7562\(09\)80388-2](https://doi.org/10.1016/s0953-7562(09)80388-2)
- [53] Ghisalberti E, Hockless D, Rowland C, White A (1993) Structural study of curvularin, a cell division inhibitor. Aust J Chem 46 (4):571-575. doi: [10.1071/ch9930571](https://doi.org/10.1071/ch9930571)
- [54] Dai J, Krohn K, Flörke U, Pescitelli G, Kerti G, Papp T, Kövér KE, Béneyei AC, Draeger S, Schulz B (2010) Curvularin-Type Metabolites from the fungus *Curvularia* sp. isolated from a marine alga. Eur J Org Chem 2010 (36):6928-6937. doi: [10.1002/ejoc.201001237](https://doi.org/10.1002/ejoc.201001237)
- [55] Kobayashi A, Hino T, Yata S, Itoh TJ, Sato H, Kawazu K (1988) Unique spindle poisons, curvularin and its derivatives, isolated from *Penicillium* species. Agr Biol Chem 52 (12):3119-3123. doi: [10.1271/abb1961.52.3119](https://doi.org/10.1271/abb1961.52.3119)
- [56] Meng L-H, Li XM, Lv CT, Li CS, Xu GM, Huang C-G, Wang B-G (2013) Sulfur-containing cytotoxic curvularin macrolides from *Penicillium sumatrense* MA-92, a fungus obtained from the rhizosphere of the mangrove *Lumnitzera racemosa*. J Nat Prod 76 (11):2145-2149. doi: [10.1021/np400614f](https://doi.org/10.1021/np400614f)
- [57] Azizi S, Ahmad M, Mahdavi M, Abdolmohammadi S (2013) Preparation, characterization, and antimicrobial activities of ZnO nanoparticles/cellulose nanocrystal nanocomposites. Bioresour 8 (2):1841-1851. doi: [10.15376/biores.8.2.1841-1851](https://doi.org/10.15376/biores.8.2.1841-1851)
- [58] Baruwati B, Polshettiwar V, Varma RS (2009) Glutathione promoted expeditious green synthesis of silver nanoparticles in water using microwaves. Green Chem 11 (7):926-930. doi: [10.1039/b902184a](https://doi.org/10.1039/b902184a)
- [59] Sun D, Zhang N, Xu Q-J, Luo G-G, Huang R-B, Zheng L-S (2010) A novel silver (I)-containing supramolecular framework incorporating eight different hydrogen bond motifs. J Mol Struct 969 (1):176-181. doi: [10.1016/j.molstruc.2010.02.001](https://doi.org/10.1016/j.molstruc.2010.02.001)
- [60] Tamma PD, Cosgrove SE, Maragakis LL (2012) Combination therapy for treatment of infections with gram-negative bacteria. Clin Microbiol Rev 25 (3):450-470. doi: [10.1128/cmr.05041-11](https://doi.org/10.1128/cmr.05041-11)
- [61] Sondi I, Salopek-Sondi B (2004) Silver nanoparticles as antimicrobial agent: a case study on *E. coli* as a model for Gram-negative bacteria. J Colloid Interface Sci 275 (1):177-182. doi: [10.1016/j.jcis.2004.02.012](https://doi.org/10.1016/j.jcis.2004.02.012)
- [62] Kim K-J, Sung WS, Suh BK, Moon S-K, Choi J-S, Kim JG, Lee DG (2009) Antifungal activity and mode of action of silver nano-particles on *Candida albicans*. Biometals 22 (2):235-242. doi: [10.1007/s10534-008-9159-2](https://doi.org/10.1007/s10534-008-9159-2)
- [63] Stoimenov PK, Klinger RL, Marchin GL, Klabunde KJ (2002) Metal oxide nanoparticles as bactericidal agents. Langmuir 18 (17):6679-6686. doi: [10.1021/la0202374](https://doi.org/10.1021/la0202374)
- [64] Ali SM, Yousef NM, Nafady NA (2015) Application of biosynthesized silver nanoparticles for the control of land snail *Eobania vermiculata* and some plant pathogenic fungi. J Nanomater 501:218904. doi: [10.1155/2015/218904](https://doi.org/10.1155/2015/218904)